



High-order finite difference solution of the Euler equations for nonlinear waves

Bingham, Harry B.; Christiansen, Torben Robert Bilgrav

Published in:
IWWWFB26

Publication date:
2011

Document Version
Publisher's PDF, also known as Version of record

[Link back to DTU Orbit](#)

Citation (APA):
Bingham, H. B., & Christiansen, T. R. B. (2011). High-order finite difference solution of the Euler equations for nonlinear waves. In *IWWWFB26*

General rights

Copyright and moral rights for the publications made accessible in the public portal are retained by the authors and/or other copyright owners and it is a condition of accessing publications that users recognise and abide by the legal requirements associated with these rights.

- Users may download and print one copy of any publication from the public portal for the purpose of private study or research.
- You may not further distribute the material or use it for any profit-making activity or commercial gain
- You may freely distribute the URL identifying the publication in the public portal

If you believe that this document breaches copyright please contact us providing details, and we will remove access to the work immediately and investigate your claim.

High-order finite difference solution of the Euler equations for nonlinear waves *

Harry B. Bingham and Torben B. Christiansen[†]
Mech. Engineering, Tech. Univ. of Denmark
E-mail: hbb@mek.dtu.dk, tobcb@mek.dtu.dk

Introduction

This abstract describes the application of a high-order finite difference strategy to solving the Euler equations with a free-surface. The immediate goal is to determine the computational penalty (if any) of moving from a potential flow to the Euler equations with this solution strategy. The long-term goal is to apply the strategy to nonlinear wave-structure interaction, in particular for the analysis of wave power generation devices.

The numerical solution strategy adopted here is based on that described in [1, 2] which extends the work of [4] to high-order finite difference schemes and non-uniform grid spacing. This work can, to some extent, also be seen as an extension of [5] to high-order and non-uniform grids.

We begin with an analysis of the linearized equations where, not surprisingly, the Euler equations become essentially identical to a potential flow formulation. The linear accuracy and stability properties of the Euler solver are thus also nearly identical to the potential flow solver. For nonlinear problems, ensuring an adequate level of mass conservation is critical, and we discuss several strategies for doing so in the context of explicit time-stepping schemes and the finite difference method. Finally, some preliminary results are given comparing the accuracy of the solution to a potential flow solver for highly nonlinear periodic wave solutions based on stream function theory.

Formulation

A Cartesian coordinate system is adopted with the xy -plane located at the still water level and the z -axis pointing upwards. The still water depth is given by $h(x, y)$ and the position of the free surface is defined by $z = \zeta(x, y, t)$; the gravitational acceleration $g = 9.81m^2/s$ is assumed to be constant. Indicical notation is invoked with $x_i = [x_1, x_2, x_3]$ and $u_i = [u_1, u_2, u_3]$; thus the summation convention applies to repeated indices. For an inviscid and incompressible fluid with density ρ , conservation of mass and momentum are expressed by the Euler equations:

$$\partial_i u_i = 0 \tag{1a}$$

$$\partial_t u_i = -\partial_j (u_i u_j) - \frac{1}{\rho} \partial_i p. \tag{1b}$$

where ∂_i denotes differentiation with respect to x_i . Here the total fluid pressure P has been split into static and dynamic components:

$$P = p_s + p, \quad \text{with} \quad p_s = -\rho g x_3. \tag{2}$$

On the free surface we ignore the atmospheric pressure and set the total pressure to zero, and impose the usual kinematic condition

$$\partial_t \zeta = u_3 - u_1 \partial_1 \zeta - u_2 \partial_2 \zeta, \quad \text{on } x_3 = \zeta \tag{3a}$$

$$p = \rho g \zeta, \quad \text{on } x_3 = \zeta \tag{3b}$$

On solid boundaries we enforce the free-slip conditions

$$n_i u_i = 0, \quad n_i \partial_i p = 0, \tag{4}$$

*The authors wish to thank the Danish Agency for Science, Technology and Innovation (grant # 09-067257) for funding, and the Danish Center for Scientific Computing for supercomputing resources.

[†]Presenting author

with n_i the unit normal vector to the boundary.

The momentum equations (1b) and the kinematic free-surface condition (3a) provide evolution equations for each component of velocity and the surface elevation, while the pressure is constructed to ensure satisfaction of the continuity equation. Thus taking the divergence of the momentum equations gives a Poisson-type equation for the pressure

$$\partial_i (\partial_i p) = -\rho \partial_i [\partial_t u_i + \partial_j (u_i u_j)]. \quad (5)$$

Note that we do not manipulate this equation further before replacing the continuous differential operators with discrete ones since we must ensure continuity on the discrete level. This point is discussed further below.

Numerical Solution

Following the references cited in the introduction, we employ a method-of-lines approach in which the Euler equations (1a)-(1b) and kinematic free surface condition (3a) are discretized in space using high-order finite difference schemes on collocated grids, while a suite of explicit Runge-Kutta type schemes are applied for the time-stepping, as detailed below. The time-varying physical domain is mapped to a fixed computational space which is discretized using one arbitrarily spaced set of points along each dimension. One-dimensional finite difference schemes of order p are developed in each direction using $p + 1$ neighbors to each grid point. The schemes are off-centered as they approach boundaries to include only the available grid points. Along solid boundaries an extra computational point is included outside the physical domain to allow enforcement of both the field equation and the boundary condition at all boundary points. The addition of extra computational points at the free surface, in order to satisfy both the Poisson equation and the Dirichlet boundary condition, is also an option. This allows all the continuous spatial derivatives to be approximated discretely. The Poisson problem is solved using a preconditioned GMRES method with the linearized $p = 2$ matrix as the preconditioner. The implementation is only 2D at this point, and the preconditioning step is done using a direct sparse matrix factorization.

The linear solution

For small amplitude waves, the problem can be linearized to obtain

$$\partial_t u_i = -\frac{1}{\rho} \partial_i p \quad (6a)$$

$$\partial_i (\partial_i p) = \partial_i (\partial_t u_i) \quad (6b)$$

$$\partial_t \zeta = u_3, \quad \text{on } \zeta = 0 \quad (6c)$$

$$p = \rho g \zeta, \quad \text{on } \zeta = 0. \quad (6d)$$

Linearization de-couples the velocities in the bulk of the fluid which become purely forced by the vertical velocity on the free-surface and the surface elevation via the pressure. The flow is thus essentially identical to a potential flow solution. Fourier analysis of the linearized system gives very similar results to that shown by [1, 2]. An example of the accuracy of computing u_3 on the free-surface from the linear ζ is shown in Figure 1.

The nonlinear solution

In the nonlinear case, special care is required to avoid accumulation of errors in mass conservation when using finite differences and explicit time-stepping. The approach we are pursuing seeks to satisfy the continuity equation in discrete form by consistently deriving the discrete Poisson equation for the pressure from the discrete momentum equations. This procedure can be illustrated

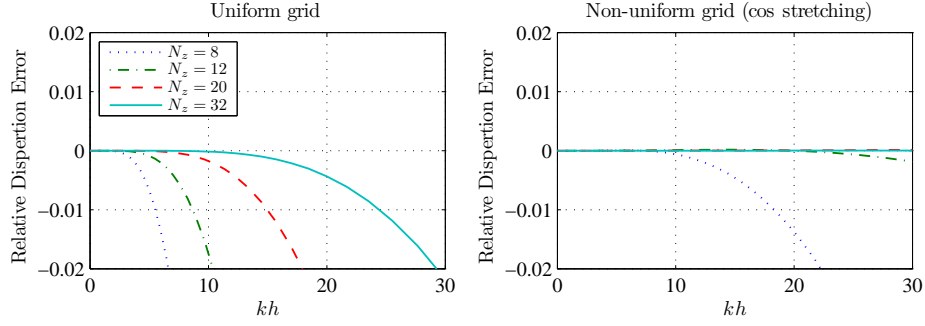


Figure 1: Linear dispersion errors as a function of relative water depth kh for sixth-order spatial finite difference schemes at several resolutions in the vertical and $N_x = 16$ points per wavelength.

by considering the explicit TVD (Total Variation Diminishing) RK33 scheme of [3] applied to the momentum equations

$$u_i^{(1)} = u_i^{(m)} + \Delta t L(u_i^{(m)}) \quad (7a)$$

$$u_i^{(2)} = \frac{3}{4}u_i^{(m)} + \frac{1}{4}u_i^{(1)} + \frac{1}{4}\Delta t L(u_i^{(1)}) \quad (7b)$$

$$u_i^{(m+1)} = \frac{1}{3}u_i^{(m)} + \frac{2}{3}u_i^{(2)} + \frac{2}{3}\Delta t L(u_i^{(2)}) \quad (7c)$$

where $u_i^{(m)}$ represents the discrete velocity field at time step m , $u_i^{(1)}$, $u_i^{(2)}$ are intermediate stage values and $L(u_i)$ represents the discrete evaluation of the right hand side of (1b) using velocity field u_i . The kinematic free surface condition (3a) is also advanced in time using the same TVD-RK33 scheme. Noting that the discrete differential operators are time dependent and functions of ζ , we define $\delta_i^{(m)}$ to be the discrete derivative operator in the direction i corresponding to the surface elevation $\zeta^{(m)}$. Given the solution $(\zeta^{(m)}, u_i^{(m)})$ at time step m , we move to the first stage by first evaluating the new free surface elevation

$$\zeta^{(1)} = \zeta^{(m)} + \Delta t \left(u_3^{(m)} - u_1^{(m)} \delta_1^{(m)} \zeta^{(m)} - u_2^{(m)} \delta_2^{(m)} \zeta^{(m)} \right) \quad (8)$$

which allows the new differential operators $\delta_i^{(1)}$ to be formed. Now taking the discrete divergence of (7a) gives

$$\delta_i^{(1)} u_i^{(1)} = \delta_i^{(1)} u_i^{(m)} + \Delta t \left[-\delta_i^{(1)} \delta_j^{(m)} (u_i^{(m)} u_j^{(m)}) - \frac{1}{\rho} \delta_i^{(1)} \left(\delta_i^{(m)} p^{(m)} \right) \right]. \quad (9)$$

To ensure that the new velocity field is divergence free, we set $\delta_i^{(1)} u_i^{(1)} = 0$ which gives

$$\delta_i^{(1)} \left(\delta_i^{(m)} p^{(m)} \right) = \rho \left[-\delta_i^{(1)} \delta_j^{(m)} (u_i^{(m)} u_j^{(m)}) + \frac{1}{\Delta t} \delta_i^{(1)} u_i^{(m)} \right] \quad (10)$$

as the Poisson equation for the pressure which ensures a divergence free velocity field $u_i^{(1)}$ at the first stage. After solving for $p^{(m)}$, (7a) is used to move the velocity field to the first stage and the procedure is repeated at the second stage and so on. This approach is applicable to any explicit time-stepping scheme.

The approach discussed above combines explicit time integration of the discrete momentum equations with implicit satisfaction of the discrete continuity equation, in which the discrete divergence and gradient operators used in the Poisson equation (10) must be consistent with those used in the discrete continuity and momentum equations. Alternatively we may approximate the discrete Laplacian of the pressure by compact finite differences, *i.e.* using $\delta_{ii}^{(m)} p$ instead of $\delta_i^{(1)} (\delta_i^{(m)} p)$ in (10), which though inconsistent is a common approach, followed *e.g.* by [5].

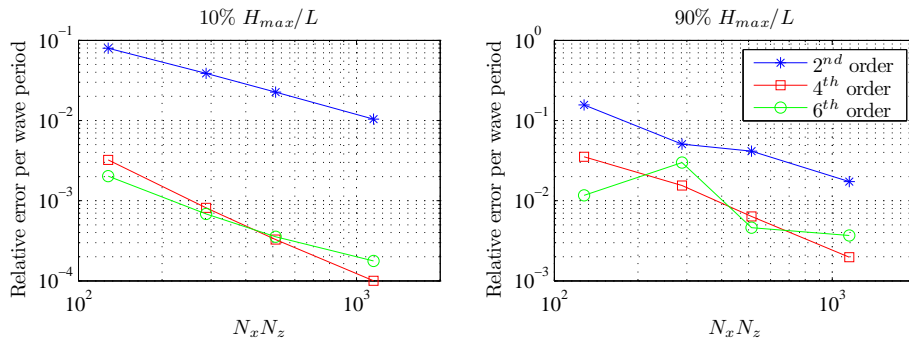


Figure 2: Errors for nonlinear traveling waves.

The model has so far been implemented in two dimensions with periodic boundary conditions in x in order to validate the model against the stream function solution for traveling waves of constant form. We find that solving for the pressure from (10) leads to machine precision errors in discrete continuity at all grid points in the domain except those at the free surface, where the Poisson equation has been replaced with the dynamic free surface condition (3b). At the free surface, the discrete continuity errors are found to grow in time, eventually leading to instability. One remedy to this problem is to introduce an extra computational point above the free surface, in order to satisfy both the Poisson equation and the Dirichlet boundary condition for the pressure at the free surface. However, we have so far found that this combination leads to a poorly conditioned problem which can not be solved robustly.

In contrast, the combination of the compact Laplacian operator $\delta_{ii}p$ and extra computational points above the free surface has been found to bound the continuity errors in time and work well for a wide range of nonlinear waves. A benchmark case with wave number $kh = 2$, Courant number $C_r = 0.5$ and wave steepnesses of respectively 10 and 90 % of the theoretical limiting steepness has been advanced in time using the TVD-RK33 scheme. The relative error per wave period in the surface elevation measured after five periods is presented in Figure 2 for uniform grid resolutions of $(N_x, N_z) = (16, 8), (24, 12), (32, 16), (48, 24)$. For the 10% case the errors are in accordance with the linear accuracy analysis in Figure 1 and on level with the results in [1].

At IWWF26 we expect to present a solution to the problem of solving the Poisson equation for the pressure consistently with additional computational points above the free surface, and further present results obtained with the model for some preliminary wave-structure interaction problems.

References

- [1] H. B. Bingham and H. Zhang. On the accuracy of finite difference solutions for nonlinear water waves. *J. Engineering Math.*, 58:211–228, 2007.
- [2] A. P. Engsig-Karup, H. B. Bingham, and O. Lindberg. An efficient flexible-order model for 3D nonlinear water waves. *J. Comput. Phys.*, 228:2100–2118, 2009.
- [3] S. Gottlieb and C.-W. Shu. Total variation diminishing Runge-Kutta schemes. *Mathematics of Computation*, 67(221):73–85, 1998.
- [4] B. Li and C. A. Fleming. A three-dimensional multigrid model for fully nonlinear water waves. *Coastal Engineering*, 30:235–258, 1997.
- [5] B. Li and C. A. Fleming. Three-dimensional model of Navier-Stokes equations for water waves. *J. Port Waterway Coastal & Ocean Eng.*, 127(1):16–25, 2001.